ACS AGRICULTURAL SCIENCE & TECHNOLOGY

pubs.acs.org/acsagscitech

Article

Plant Viral Nanocarrier Soil Mobility as a Function of Soil Type and Nanoparticle Properties

Udhaya Pooranam Venkateswaran,◆ Adam A. Caparco,◆ Ivonne González-Gamboa, Reca Marian Caballero, Juliane Schuphan, and Nicole F. Steinmetz*

Cite This: https://doi.org/10.1021/acsagscitech.3c00074

Read Online

ACCESS | Metrics & More | Article Recommendations

ABSTRACT: The use of nanoparticles for agrochemical delivery is an important step toward achieving global food security. Specifically, the ability to target the delivery of pesticides and other useful chemicals into the soil will greatly improve the efficiency and efficacy of these molecules, mitigating crop losses associated with pests and parasitic organisms. While synthetic nanoparticles can be a good delivery vehicle and demonstrate high mobility in the soil, their fate and persistence have some implications for human and environmental health. Therefore, using proteinaceous materials such as plant virus nanoparticles, which have already been adapted for the soil, provides a fruitful avenue of exploration. Previously, tobacco mild green mosaic virus (TMGMV) and red clover necrotic mosaic virus (RCNMV) have shown high soil mobility and nematicide delivery for the treatment of plant parasitic nematodes. To further the use of these plant virus nanoparticles in soil delivery applications, understanding the properties of the soil and the nanoparticles is essential. In this work, we assessed the mobility of TMGMV, potato virus X, and tobacco mosaic virus with a genetically encoded lysine on its surface (TMV-Lys) and virus-like particles of physalis mottle virus (PhMV) in four types of soil. The particles were loaded in a cylindrical column of soil, eluted, and analyzed for the protein signal. A mathematical model was used to compare their relative mobility. Data indicate that TMGMV has higher soil mobility compared to the other plant virus-based nanoparticles analyzed, and this appeared to be independent of the soil environment. Data indicate that the presence of a high-density lysine corona may not be favorable for soil applications. While this work provides insights into nanoparticle design rules for soil applications, data also highlight that more systemic studies are needed to delineate the design rules for soil delivery of nanocarriers.

KEYWORDS: *food security, nanotechnology and agriculture, plant virus nanoparticle, soil mobility, pesticide delivery*

INTRODUCTION

The demand for food is increasing with the exponentially growing population. Be it for animal or human consumption, basic food security is a concern with limited resources and increased demand for food crops (the World Food Program[1]). Due to this surge in demand, pesticides, fertilizers, and anti-weed control measures have been extensively used in the current agricultural setup to achieve two main objectives: increased yield and control of soil conditions for future use. However, the extensive use of pesticides in agriculture causes these toxins to accumulate on crops, in soil, and in drinking and groundwater, severely endangering the ecosystem and human health.[2] The first step toward a healthier society is to enhance food security by improving quality and yields (i.e., more effective crop treatment) while protecting the environment and agricultural ecosystems (i.e., preventing the leaching and accumulation of pesticides in the environment).

Precision farming through nanotechnology is an area that has gained attention in recent years.[3] For example, nanocarriers have been proposed to deliver genetic material to plants to enhance plant function by providing resistance to pathogens and environmental threats.[4] Nanoparticle-formulated fertilizers have also been used to enhance absorption and controlled delivery of nutrients in plants.[5,6] We[7] and others[8] have focused on the development of nanocarriers for controlled delivery of pesticides to the rhizosphere. The promise of nanotechnology is the controlled and targeted delivery of cargo,[8,9] like human nanomedicines.[10] Nanomaterials as carriers have advantages over free pesticides applied in the field; when pesticide-loaded nanoparticles are spread uniformly over the soil surface, their large surface area increases their affinity for the target pest and reduces the dose required for eradication.[11] Furthermore, the encapsulation of pesticides in nanoparticles protects the active compound from premature biodegradation and photolysis and limits or prevents end-user exposure. Liposomal and polymer-based nanoparticle formulations have already been used as pesticide delivery systems.[8] Although synthetic nanomaterials overcome some challenges associated with the use of nematicides, they may be too expensive for routine use.[8] More importantly, biodegradability and safety issues must be

Received: March 9, 2023
Revised: May 26, 2023
Accepted: May 30, 2023

addressed when introducing synthetic materials into the environment.[12]

We propose plant virus-based pesticide nanocarriers as an economically and environmentally viable alternative to synthetic nanoparticles. The application of plant virus-based nanocarriers to crops may initially appear counterintuitive because plant viruses infect and damage crops. However, plant viruses can be rendered noninfectious toward plants by means of the use of virus-like particles devoid of their genome[13] or through viral inactivation.[14,15] Plant virus nanoparticles can be produced in large quantities (i.e., 500 mg virus in 100 g leaves) using fast and cost-effective molecular farming.[16] The biological nanoparticles offer a high level of sophistication and unparalleled engineering design space; plant viruses come in many shapes and sizes, and their size and shape can be precisely tailored through programmed bottom-up design yielding rods, spheres, and stellate and falcate structures.[17] These biological materials offer the highest level of quality control and assurance, and reproducibility is ensured by the fact that each particle is genetically encoded, yielding highly uniform preparations. Production is scalable through farming in plants. Given that viruses have naturally evolved to protect and efficiently deliver their payload (i.e., their genome), they can be regarded as naturally occurring nanocarriers. Plant viruses are biodegradable, yet they are exceptionally robust in the harsh open-field environment. Finally, and most importantly, from a human health perspective, plant viruses are biocompatible and noninfectious to mammals, making them safe to use on food and feed crops.

In this work, we set out to analyze the soil mobility properties of plant viruses. In prior work, we have shown that the high aspect ratio nanoparticles formed by tobacco mild green mosaic virus (TMGMV) exhibit superior soil mobility when compared to synthetic polymeric nanoparticles or inorganic silica nanoparticles.[18] Others have demonstrated the application of red clover necrotic mosaic virus (RCNMV) for nematicide delivery to plants.[9] The 30 nm icosahedral RCNMV particles efficiently encapsulate hydrophobic drugs using a salt/pH gating mechanism, and in an agricultural setting, the effective treatment of tomato seedlings infested with the root-knot nematode *Meloidogyne hapla* was demonstrated using RCNMV particles carrying abamectin. Encapsulated abamectin significantly reduced the size of nematode galls compared to the free drug and virus alone. These prior works highlight the potential of plant virus nanotechnology for agricultural applications. Toward structure−function studies guiding the design or tailor-made nanocarriers for soil applications, we set out to analyze the soil mobility of TMGMV and compare it with other plant virus nanoparticles of varying sizes and shapes using different soils as a testbed.

METHODS

Soil Analysis by Western Laboratories. A comprehensive soil analysis was conducted for each soil by Western Laboratories (Parma, Idaho). Magic topsoil (#5540) was purchased from Michigan Peat Co (Sandusky, MI), and veggie, potting, and 50/50 soils were provided by SoCal Mulch (Menifee, CA).

Purification of Plant Virus Nanoparticles. The United States Department of Agriculture permits (P526P-21-02414) were obtained for any work with plant viruses. TMGMV was procured from BioProdex (Gainesville, FL) and stored at 20 °C until further purification. Frozen TMGMV was thawed at 4 °C overnight and then dialyzed against potassium phosphate buffer (KP; 10 mM, pH 7.2) for 24 h at 4 °C using 12−14 kDa dialysis tubing (Fisher Scientific S432700; Waltham, MA). The buffer solution was replaced, and the dialysis continued for an additional 48 h. The solution was then centrifuged at 10,000*g* for 20 min (Beckman Coulter Allegra or Avanti centrifuges). The supernatant was collected and ultracentrifuged at 120,000*g* for 2.5 h at 4 °C (Beckman Coulter OptimaL-90k Ultracentrifuge with 50.2 Ti rotor; Brea, CA). The pellet was resuspended under rotational mixing overnight at 4 °C in KP buffer. The sample concentration was then confirmed using a Nanodrop 2000 (Thermo Scientific; Waltham, MA); the concentration was adjusted to 10 mg mL^{-1} in 10 mM KP before storing at 4 °C (for TMGMV CP, ε_{260} = 3 mL mg^{-1} cm^{-1}). Tobacco mosaic virus lysine mutant (TMV-Lys),[19] potato virus X (PVX), and virus-like particles of physalis mottle virus (PhMV) were purified as previously described[20,21] and stored in 10 mM KP or sodium citrate buffer at 4 °C.

Transmission Electron Microscopy (TEM). Samples were diluted to 0.05 mg mL^{-1} in DI water and absorbed onto carbon-coated TEM grids (Electron Microscopy Sciences, Hatfield, PA). The grids were then washed three times with DI water. Then, grids were stained with 2% (w/v) uranyl acetate (Fisher Scientific; Waltham, MA) for 2 min for imaging. TEM was conducted using an FEI Tecnai F30 transmission electron microscope operated at 300 kV.

Zeta Potential Measurement. TMGMV was diluted to 0.01 mg mL^{-1} in DI water and 10 μL was loaded into the DTS1070 cuvette with the remaining volumes filled with DI water. Zeta (ζ) potentials were measured using the Zetasizer NanoZS (Malvern Panalytical; Westborough, MA). Measurements were run in triplicate (N = 3) and expressed as the ζ potential (mV) ± standard deviation (SD).

Soil Mobility Assay. Soil columns were made from 50 mL Falcon tubes with the bottom end cut. The bottom ends were covered with two layers of 2.5" cheesecloth to filter soil particulates. Water-saturated soil was packed into the column from the top using a spatula. For soil mobility studies, plant virus nanoparticles were applied to the soil columns from the top using a syringe pump at a constant flow rate of 5.0 mL min^{-1}, and fractions were collected using 0.5 and 2 mL tubes for protein quantification. The collected soil eluent was centrifuged for 15 s to remove sediments, and the supernatant was collected and stored at 4 °C until characterization by a BCA assay or SDS-PAGE. Measurements were made in triplicate (N = 3).

Bicinchoninic Acid (BCA) Protein Assay. A 1:8 dilution of the eluent was used in a BCA assay, and the working reagent was made in the ratio of 1:9 according to the manufacturer's protocol (Thermo Fischer Scientific; Waltham, MA). Samples were run in triplicate (N = 3). Using a Tecan (Infinite 200Pro) plate reader, sample absorbance was measured at 562 nm wavelength and compared to a standard curve of bovine serum albumin.

SDS-PAGE. Collected fractions (1:8 dilution) from soil columns were analyzed by SDS-PAGE using a NuPAGE 4−12% Bis-Tris protein gel and 1× MOPS buffer (Fisher Scientific; Waltham, MA). Proteins were separated at 200 V and 120 mA for 35 min. Gels were stained with Coomassie brilliant blue and imaged using a FluorChem R system (Protein Simple, bio-techne, Minneapolis, MN), followed by lane analysis using ImageJ software (https://imagej.nih.gov/ij/download.html).

RESULTS AND DISCUSSION

Composition of Magic Topsoil (MTS), Veggie, Potting, and 50/50 Soils. Based on our prior work,[18] investigating the soil mobility of plant virus nanoparticles and synthetic nanoparticles, MTS was selected as an exemplar soil for this work. MTS is intended to be applied as a universal topsoil; it is composed primarily of sedge peat and sand, giving it a relatively high organic content. However, in the agricultural setting, soil composition varies from that of MTS. To understand the effect of soil composition on plant viral nanoparticle mobility, three soils composed of the same base components at different ratios were selected. The shorthand

https://doi.org/10.1021/acsagscitech.3c00074
ACS Agric. Sci. Technol. XXXX, XXX, XXX−XXX

(A)

Soil Type	pH	Soluble Salts	NO_3 (ppm)	NH_4 (ppm)	P (ppm)	K (ppm)	Ca (ppm)	Mg (ppm)	S (ppm)	Na (ppm)	Zn (ppm)	Cu (ppm)	Mn (ppm)	Fe (ppm)	B (ppm)
Magic Top	6	0.3	1	6	10	70	128	18	91	23	4.1	1	11.2	5.5	0.3
Veggie	6.3	1	24	30	10	333	470	194	758	202	8.2	0.7	24.5	19.1	1.6
Potting	6.6	1.8	11	35	9	303	427	168	832	206	7	0.9	21.8	19.8	1.4
50-50	6.7	2.2	3	25	11	274	524	223	1002	267	9.1	1.8	40.8	36.6	1.6

(B)

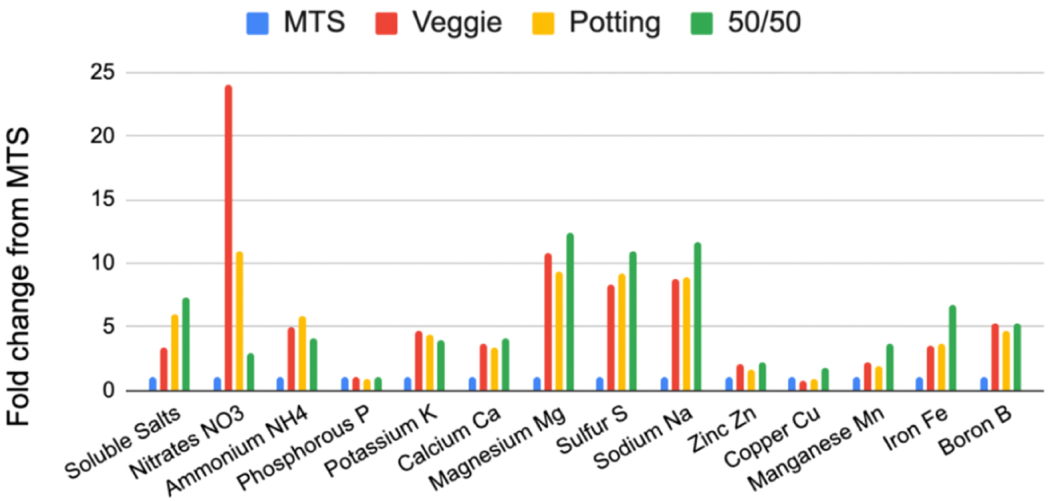

Figure 1. Chemical composition of various soil types is distinct. Analysis was performed by Western Laboratories, and chemical composition in ppm of MTS, veggie, potting, and 50/50 soils is tabulated in panel A. Panel B shows that veggie, potting, and 50/50 soils are generally more nutrient-rich compared to MTS soil; fold change over MTS is plotted.

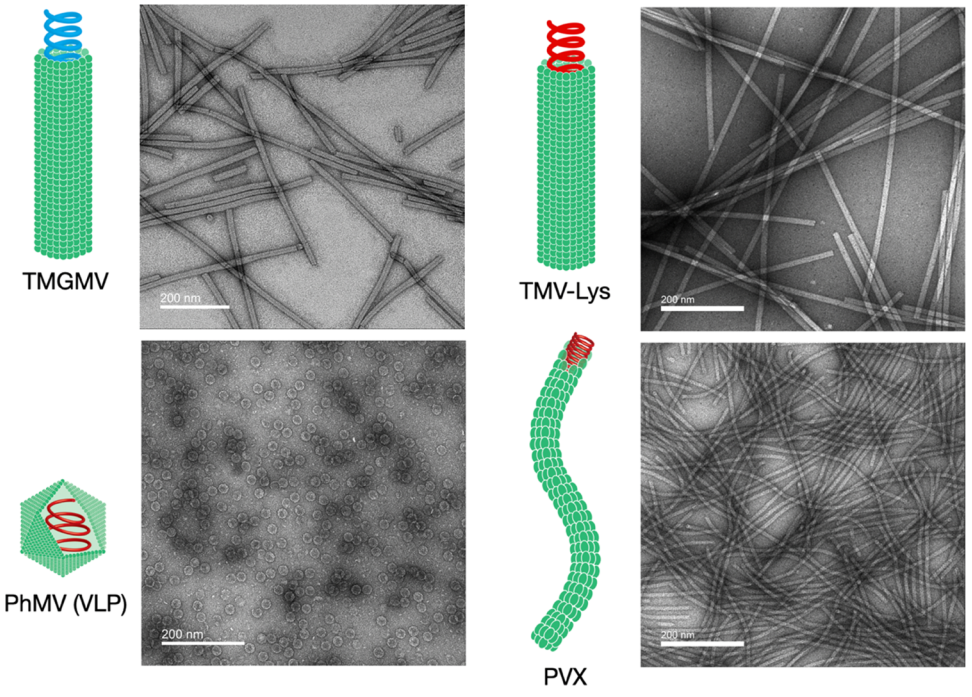

Figure 2. TEM images of negatively stained plant virus nanoparticles.

names of these soil blends are potting, veggie, and 50/50, in the order of increasing filler content. These soils are composed primarily of silt, sand, and clay (soil blend) with a proprietary filler added. All three of these soils appeared finer and more granular than MTS, which is composed primarily of peat. The average particle size is visibly smaller with increasing filler concentration, and 50/50 feels silty and oily to the touch. The composition of sand seems to decrease with increasing filler concentration, as potting and 50/50 have slower draining of water than MTS or veggie.[22]

To understand any differences in the chemistry of these soils, the composition of the soils was analyzed by Western Laboratories, highlighting differences between the soils (Figure 1). Veggie, potting, and 50/50 soils are, in general, significantly more nutrient-rich than MTS; 50/50 is the most nutrient-rich soil type based on high levels of sodium, sulfur, magnesium, and iron, while veggie soil contains the highest amounts of

https://doi.org/10.1021/acsagscitech.3c00074
ACS Agric. Sci. Technol. XXXX, XXX, XXX−XXX

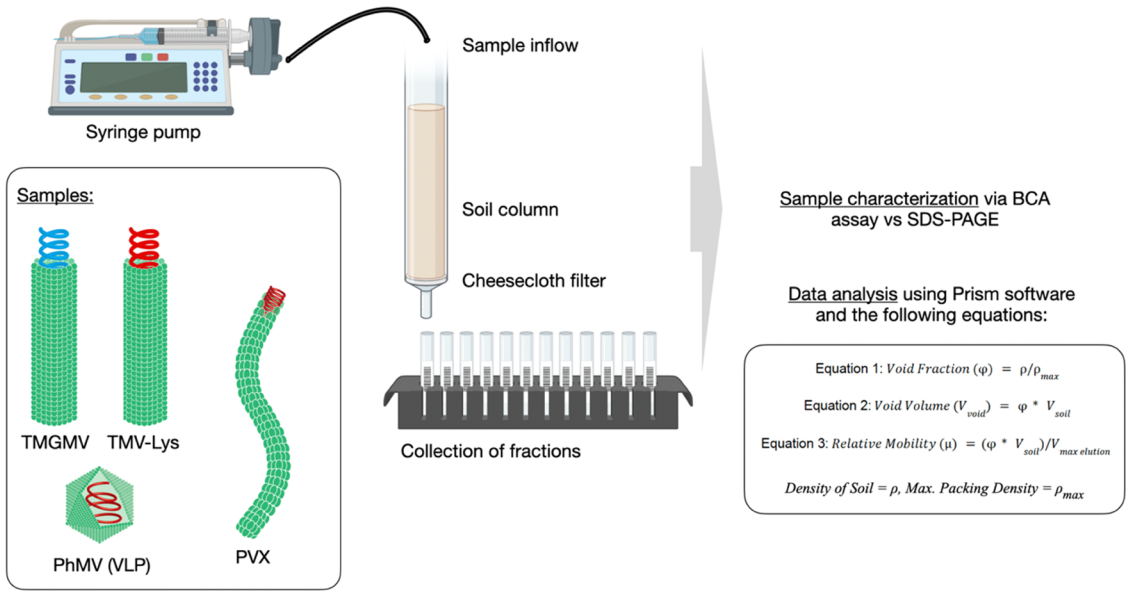

Figure 3. Experimental overview. The following samples were analyzed for soil mobility using MTS, veggie, potting, and 50/50 soils packed into a soil column; virus nanoparticles (TMGMV, TMV-Lys, PVX, and PhMV (VLPs)) were applied onto the soil column at a consistent flow rate (5 mL/min) using a syringe pump. The outflow was filtered using cheesecloth to trap larger soil particulates; fractions were collected and subjected to protein analysis to determine the soil mobility of the virus nanoparticles. The figure was created using BioRender.com.

nitrates (NO_3). Veggie and potting are designed for growing vegetables and seedlings, whereas 50/50 is formulated for more general landscaping purposes. The pH of each of these soils is below 7, which is appropriate for TMGMV to maintain its structure. The physical and chemical differences of these soils provide a framework for probing the effects of soil composition on the mobility of several plant viral nanoparticle formulations.[23]

Properties of Plant Virus Nanoparticles. We chose the following plant virus nanoparticles for this study: the nucleoprotein assemblies of TMGMV and TMV-Lys forms rigid nanotubes measuring 300 × 18 nm. TMGMV and TMV are closely related with their coat proteins exhibiting >70% amino acid sequence similarity (UniprotIDs: TMGMV-P03579 and TMV-P69687).[24] A key difference is the surface charge of TMGMV vs the TMV-Lys mutant; the latter was genetically engineered to display a corona of lysine resides at the solvent-exposed C-terminus of the coat protein (a threonine to lysine substitution at the amino acid position 158).[19] While TMV has an overall negative surface charge (wild-type TMV has a ζ potential of $\zeta \sim -18$ mV), the lysine residue renders TMV-Lys more closely neutrally charged with a ζ potential of ζ −8 mV.[25] We measured the ζ potential of TMGMV and found that it was similar to TMV-Lys with $\zeta = -6.43 \pm 1.15$ mV. While the ζ potential is not significantly different, a key difference remains the corona of positively charged Lys-side chains extending from the surface of TMV-Lys. We note that TMV-Lys was chosen for this work as opposed to TMV because our initial goals were to also assess a number of chemically modified TMV-Lys, including those that are charge neutralized. To date, data were inconclusive and these data will be reported elsewhere in the future. For our structure−function studies, we also selected potato virus X (PVX), which forms a flexuous filamentous nanoparticle measuring 515 × 13 nm and an overall positive surface charge ($\zeta \sim +25$ mV).[26] Lastly, we considered virus-like particles (VLPs) from physalis mottle virus (PhMV); these icosahedral structures form sphere-like nanoparticles with a diameter of 30 nm and a close-to-neutral yet positive surface charge ($\zeta \sim +4$ mV).[20]

TMGMV was obtained from BioProdex and further purified (see methods); TMV-Lys and PVX were produced and purified from *Nicotiana benthamiana* plants[19,21] and PhMV VLPs were obtained through heterologous expression in *Escherichia coli*.[20] The size and shape of the purified plant virus nanoparticles were verified by transmission electron microscopy (TEM), showing the characteristic rigid rods for TMGMV and TMV-Lys, flexuous filamentous nanoparticles for PVX, and spherical nanoparticles for the PhMV VLPs (Figure 2).

Experimental Setup to Assay the Soil Mobility of Plant Virus Nanoparticles. The experimental workflow is shown in Figure 3. Plant virus nanoparticles were subjected to soil columns of varying lengths with various soil types at a consistent flow rate of 5 mL/min; the outflow was filtered using cheesecloth to trap larger soil particulates; fractions were collected and subjected to protein analysis to determine the soil mobility of the virus nanoparticles. The soil mobility of TMGMV was analyzed as a function of soil type, and we also analyzed soil mobility as a function of plant virus nanoparticles in different soil types.

The fractions were analyzed for protein content by BCA and SDS-PAGE (see below), and soil mobility was calculated using the following equations

$$\textit{Void Fraction}(\varphi) = \rho/\rho_{\max} \quad (1)$$

$$\textit{Void Volume}(V_{\text{void}}) = \varphi^{*}V_{\text{soil}} \quad (2)$$

$$\textit{Relative Mobility}(\mu) = (\varphi^{*}V_{\text{soil}})/V_{\text{maxelution}} \quad (3)$$

The maximum soil packing density ($\rho_{\max}$) was measured by filling the different soil types into the columns to reach the maximum packing of soil. The parameters void fraction (φ) and void volume (V_{void}) were then calculated based on the

https://doi.org/10.1021/acsagscitech.3c00074
ACS Agric. Sci. Technol. XXXX, XXX, XXX−XXX

density of the soil. These parameters then allowed us to calculate the relative mobility based on the maximum elution volume ($V_{maxelution}$), which was determined experimentally. It should be noted, however, that the void fraction (φ) is an overapproximation because true maximum packing density could not be achieved by hand, but this comparison is still a useful tool for making comparisons between the soil mobility at different depths of soil. The soil parameters are shown in Table 1. Potting soil packed at the highest maximum packing density ρ_{max} (g/mL), whereas unpacked 50/50 had the highest prewet density. The 50/50 soil did not absorb water well, and experiments beyond a 5 mL column could not be achieved due to the stagnation of water atop of the column, a phenomenon reported for several types of soil.[27]

Table 1. Soil Parameters

soil type	soil volume (mL)	density of prewet soil ρ (g/mL)	max. packing density ρ_{max} (g/mL)	void fraction φ	void volume V_{void} (mL)
MTS	10	0.67	0.9	0.74	7.44
	25	0.49	0.85	0.58	14.41
	50	0.42	0.86	0.49	24.42
veggie	15	0.62	1.19	0.52	7.82
potting	15	0.61	1.36	0.45	6.73
50/50	5	1.06	1.21	0.87	4.38

To assay soil mobility, outflow fractions were collected, and the protein content was quantified. In prior research, we established SDS-PAGE as a feasible method as it provides confirmation of protein identification (by size) and can be quantified by band density analysis (e.g., using band analysis tool and ImageJ software). However, SDS-PAGE is cumbersome, time-consuming, and expensive when sample sizes are large. We analyzed 4 nanoparticle formulations in 4 soil types at 3 soil depths resulting in 20−40 fractions collected depending on the soil depths; each experiment was conducted at a minimum of $N = 3$. This means that more than >4,000 samples needed to be analyzed. Typical SDS-PAGE allows us to analyze 9 samples plus a marker; hence, 100s of gels would need to be run. To overcome this, we thought to use a conventional protein quantification assay, namely, the bicinchoninic acid (BCA) assay, to measure the amount of plant virus nanoparticles per fraction. To validate the sensitivity of the assay, we compared the elution profiles obtained from BCA vs SDS-PAGE analysis of fractions collected using TMGMV and a 10 mL MTS column as the testbed (Figure 4). Overall, the elution profiles are closely aligned with either method, resulting in a maximum elution volume $V_{maxelution}$ of 4 mL. It is noted that the SDS-PAGE method is more sensitive; therefore, the area under the curve (AUC) calculation to determine the amount of protein eluted is underestimated using the AUC by the BCA method vs SDS-PAGE. Further, the BCA method does not provide any information about protein identity; therefore, SDS-PAGE may need to be considered when complex soils containing multiple protein species are analyzed. Nevertheless, we found that the BCA method is a reliable and suitable method for high throughput screening and protein quantification of plant virus nanoparticles in soil fractions.

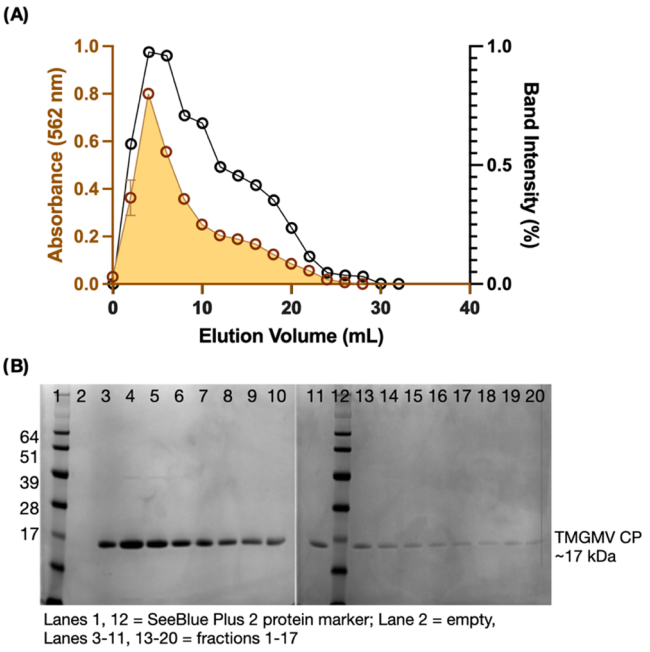

Figure 4. Comparison of the BCA assay (absorbance) vs the SDS-PAGE method (band intensity) to monitor protein elution from the soil columns. (A) Elution profile of TMGMV from a 10 mL MTS column as determined by the BCA assay (yellow) or SDS-PAGE method. (B) SDS-PAGE of 17 2 mL fractions collected from a 10 mL MTS soil column to monitor elution of TMGMV. SeeBlue Plus 2 is a protein standard, and the protein marker bands are indicated on the left in kDa. The TMGMV coat protein (CP) is detected at 17 kDa with a maximum intensity of 4 mL (as determined using a Band Analysis tool and ImageJ software).

Soil Mobility of TMGMV as a Function of Soil Type. TMGMV nanoparticles were subjected to soil columns using MTS soil with volumes of 10, 25, and 50 mL, which corresponds to approximately 2.5, 5, and 10 cm depths of soil. It is relevant to assay soil mobility at varying depths to understand whether groundwater washout effects would be likely or whether there are limitations in which depth could be reached. The rhizosphere for different crops is distinct, with shallow-rooted, moderate-rooted, and deep-rooted crops. In the laboratory setting, as a first step, we focused on shorter columns as a model for shallow root systems. Consistent with our previously published data, TMGMV exhibits good soil mobility in MTS and elutes from the 10, 25, and 50 mL MTS soil columns (Figure 5a,b). The elution peak shifts correlate with the increase in column volume, as it takes more eluent to pass the virus sample through a larger depth of soil. TEM micrographs were taken at the elution maxima for each condition, confirming the presence of intact TMGMV (Figure 5c). The particles seem to have acquired different coronas after passing through each soil type, suggesting the surface chemistry or grain size of the soil may affect how they interact with TMGMV.

The AUC calculations indicate that elution from the short 10 mL column is incomplete, and higher TMGMV recovery is achieved with the 25 and 50 mL columns. More shallow soil columns may be more susceptible to incomplete packing and formation of channels, which shift the apparent mobility of the nanoparticles in the soil.[18,22,27] Additionally, these channels and changes in the cross-section of the flowing water may lead to changes in the interactions between the soil and the nanoparticles, which could cause apparent higher retention of the nanoparticles in the soil.[28,29] This effect becomes less apparent at higher soil volumes. A decrease in the apparent

https://doi.org/10.1021/acsagscitech.3c00074
ACS Agric. Sci. Technol. XXXX, XXX, XXX−XXX

(A)

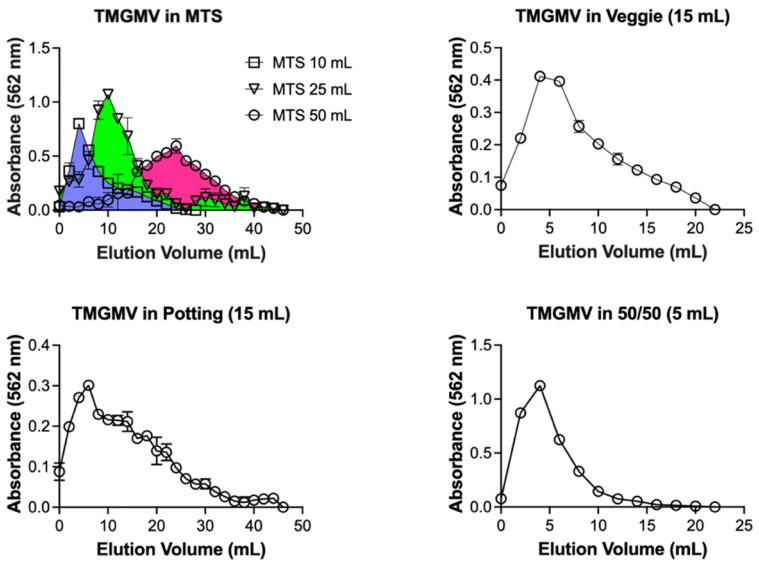

(B)

	MTS 10 mL	MTS 25 mL	MTS 50 mL	Veggie 15 mL	Potting 15 mL	50/50 5 mL
Elution volume (peak)	4	10	24	4	6	4
Area under the curve	6	12	10	4	5	7
Rel. soil mobility (Eq. 3)	1.86	1.44	1.02	1.95	1.12	1.57

(C)

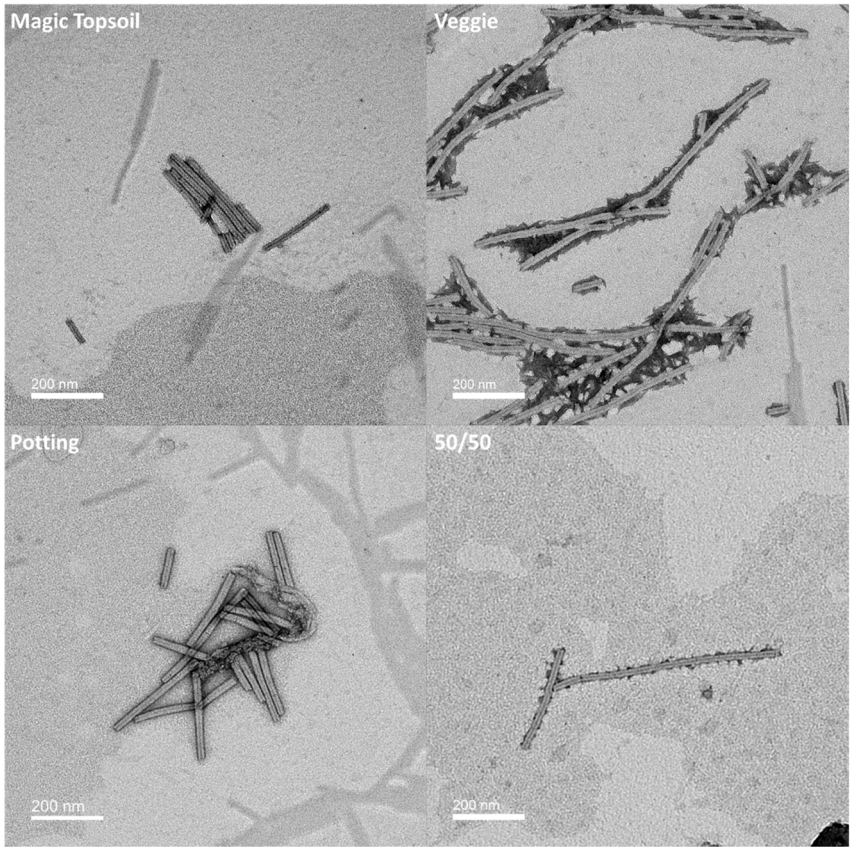

Figure 5. Soil mobility of TMGMV varies as a function of soil type. (A) Elution profile of TMGMV from MTS, veggie, potting, and 50/50 soils using 10, 25, and 50 mL columns for MTS, a 15 mL column for veggie and potting, and a 5 mL column for 50/50 soil. Triplicate experiments were performed, and averages and standard deviations are shown. (B) Elution volume, the area under the curve (AUC), and the soil mobility of TMGMV are tabulated for each soil condition. (C) TEM micrographs taken from the elution maxima of the profiles in panel (A) at 40k magnification; images show intact TMGMV.

https://doi.org/10.1021/acsagscitech.3c00074
ACS Agric. Sci. Technol. XXXX, XXX, XXX−XXX

(A) Soil mobility of virus nanoparticles

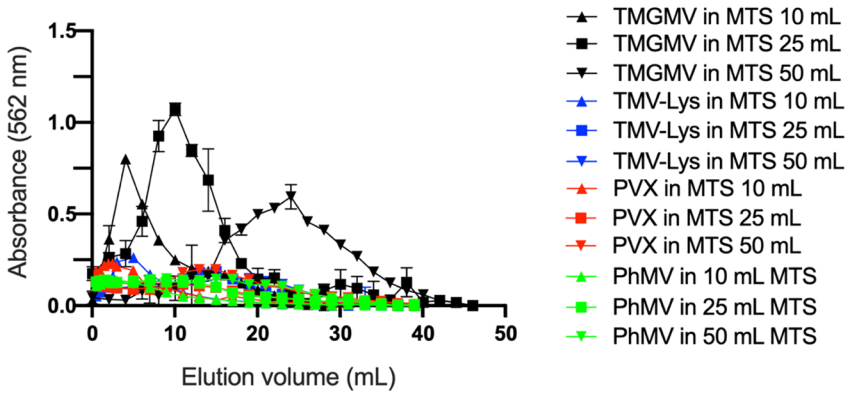

(B) Area under the curve (AUC) table

	MTS 10 mL	MTS 25 mL	MTS 50 mL	Veggie 15 mL	Potting 15 mL	50/50 5 mL
TMGMV	6	12	10	4	5	7
TMV-Lys	2.25	3.09	3.45	3.9	3.68	2.88
PhMV	1.6	2.7	3.6	2.4	3	2.3
PVX	2.3	2.2	3.9	4.1	2.8	3.3

Figure 6. TMGMV has superior soil mobility compared to other plant virus nanoparticles. (A) Elution profile of TMGMV, TMV-Lys, PVX, and PhMV (VLPs) from MTS soil using 10, 25, and 50 mL columns. Triplicate experiments were performed, and averages and standard deviations are shown. (B) Area under the curve (AUC) calculations (average values) from soil mobility experiments comparing different virus nanoparticles eluting from different soil columns.

value of the relative mobility across multiple soil depths may be explained by the variance of the elution profiles. As the soil depth increases, so does the length of the tails of the elution profile. Because the relative mobility parameter is calculated using the peak of the elution profile, the errors associated with this approximation can increase with soil depth, similar to dispersion effects seen in column chromatography.[30] It is worth noting this may be a fundamental limitation of soil columns for the soil volume, the mass of the added protein, and the water flow rate tested, but these effects could be mitigated with further optimization of these parameters in the experimental setup.

We compared elution profiles of TMGMV from veggie and potting soils using 15 mL columns. The AUC calculation indicates that about the same amount of TMGMV was recovered from the veggie and potting soil-filled columns; however, TMGMV eluted over 48 mL ($V_{maxelution}$ at 4 mL) from the potting soil vs 24 mL ($V_{maxelution}$ at 6 mL) from the veggie soil. Analysis of the soil parameters (see Table 1) indicates that potting soil packs at a slightly higher density and smaller void volume compared to veggie soil, which partially explains the different elution trends. The hydrophobicity of the potting soil results in a much slower flow of water through the column compared to veggie, occasionally resulting in the pooling of the liquid at higher volumes. This change in flow and physicochemical properties of the soil can result in more adsorptive interactions between the nanoparticles and the soil and less advection of the virus particles in the soil.[27,28] Taken together, all of these differences indicate that larger elution windows need to be investigated for taller soil columns, more hydrophobic soils, and more tightly packed soils. These differences should be considered in future applications of this assay.

After characterizing TMGMV mobility in different soil types, we sought to compare these conditions with other nanoparticles. Prior work in our lab has shown that TMGMV has exceptional soil mobility compared to other nanoparticles in MTS.[18] Building on this finding, we generated a set of nanoparticles to test in MTS, veggie, potting, and 50/50 soils. The set consists of plant virus nanoparticles, TMGMV, TMV-Lys, PVX, and PhMV (the latter are VLPs). As previously described, these particles vary in aspect ratio, surface charge, flexibility, and shape, all features hypothesized to have a bearing on their soil mobility. The elution profile by BCA in MTS for each of the nanoparticles is shown in Figure 6A. From the elution profiles in MTS, we see the magnitude of the peak was much lower for PVX and TMV-Lys. For PhMV, there was no discernable profile of elution. Because the BCA signal should be insensitive to the protein sequence, these differences are more likely due to more adsorption and retention of these nanoparticles in MTS.[31] These results are consistent with prior work, showing that TMGMV has exceptional mobility when compared to synthetic nanoparticles and other plant viruses.[18]

Parsing out some properties that may affect the soil mobility of these plant viruses, we consider their shape, surface chemistry, and structural rigidity. TMGMV is mildly positive, relatively rigid, and approximately 300 × 18 nm^2 in dimensions. TMV-Lys shares many of these properties but has a poorly defined elution profile and a high level of retention in the soil. This suggests the corona of lysine residues TMV-Lys has been engineered to express a significant effect on its ability to pass through the soil. PVX also has a poorly defined elution profile in MTS. PVX is longer and more flexible than TMGMV and exhibits a positive surface charge. An analysis of its sequence also shows it has many lysine residues in its coat protein. PhMV has the least detectable soil mobility, likely due to its smaller diameter and icosahedral shape. It is worth noting that PhMV also has a high number of lysine residues in its sequence, though the dominating effect on its soil mobility is likely its size.[32] Taken together, these

https://doi.org/10.1021/acsagscitech.3c00074
ACS Agric. Sci. Technol. XXXX, XXX, XXX−XXX

findings seem to suggest that surface lysine residues play a role in soil retention, but many complex interactions can occur between proteins and soil, so it is difficult to isolate the effect on the abundance of a single amino acid.[33]

Considering all of the soils in this study, we calculated the AUC for each soil and nanoparticle to determine their retention (Figure 6B). For MTS, the AUC data match well with the analysis on the elution profiles, clearly showing that TMGMV has the highest soil mobility and least retention in the soil. For PVX, PhMV, and TMV-Lys, the AUC is around 3-fold lower than TMGMV for all MTS volumes. The AUC for these particles also does not seem as dependent on soil composition as TMGMV. For TMGMV, there is around a 2-fold reduction in the AUC value for veggie, potting, and 50/50 compared to MTS. However, these AUC values remain higher than any other particles for potting and 50/50 soils. Interestingly, for 15 mL veggie, we see all of the high aspect ratio particles (PVX, TMV-Lys, and TMGMV) converge on the same AUC value. This suggests that the effects of the lysine corona dominate less in veggie soil and the aspect ratio is a more useful determinator of soil mobility. When comparing the properties of veggie to the other soils, the only unique feature is its high nitrate content. It is possible these nitrates adsorb to the particles and shield their surface chemistry during soil elution.[34] Because the exceptional mobility of TMGMV is reduced in other soils, it is also worth considering what makes MTS unique. MTS is primarily a peat-based soil and has 3-fold lower soluble salts than the other soils. It is possible that the lower salt content causes less shielding of the surface chemistry and allows the features of TMGMV's surface to dominate its movement in the soil.[35−37]

CONCLUSIONS

There is a growing interest in using nanocarriers in precision farming with the goal of enhancing food security. Nanoparticles offer the potential to deliver active ingredients in a more targeted fashion to the pathogen while minimizing environmental exposure.

In this work, we set out to quantitatively compare the mobility of several plant virus-based nanoparticles in four types of soil. To our knowledge, this is the first work to compare multiple plant virus nanoparticles in multiple types of soil. Overall, our data confirm that TMGMV has good soil mobility, which was not observed for TMV-Lys, PVX, and PhMV—a rigid rod (matching the shape of TMGMV), a flexuous filament, and an icosahedron, respectively. While TMV-Lys, PVX, and PhMV differ in shape, these nanoparticles have in common a high density of lysine side chains on their solvent-exposed surface.

To our knowledge, the only other plant viral nanoparticle system used to assess soil mobility and delivery of functional molecules is RCNMV. These nanoparticles are icosahedral with 36 nm diameter and net positive surface charge.[38] RCNMV is a soil-borne plant virus and is well adapted to have high soil mobility.[39] When delivering abamectin and rhodamine dye for the treatment of plant parasitic nematodes, these particles drastically improved the mobility of nematicides in both potting soil and sandy soil.[9] In spite of being of icosahedral shape with an overall positive charge and the presence of solvent-exposed surface lysine residues, RCNMV has good soil mobility. Therefore, our data, alongside the previously published data, highlight the need for more systematic studies to delineate the design rules for soil delivery of nanocarriers.

As part of this investigation, we developed a simple and efficient method to quantify the mobility of different protein-based nanoparticle systems in soil. Specifically, we found the BCA assay to be an efficient medium-throughput method. The results obtained via the BCA assay correlated with the mobility calculations made by SDS-PAGE—the contemporary method used. However, the BCA assay can be performed at a much larger scale and lower cost.[15] We also developed an approximated mathematical model to quantitatively compare the mobility of these particles. The differences in mobility values of these plant virus nanoparticles suggest that size and surface chemistry are both important determinants of soil mobility, but the relative contribution of these effects is dependent on the type of soil.

Along with the development of methods and models to quantify soil mobility of protein-based nanoparticles in soil, the key findings are that the soil mobility of plant virus nanocarriers varies in different soil types and TMGMV outperforms other plant virus nanoparticle systems; the underlying design rules remain elusive.

Continuing to grow the number of plant virus nanoparticles used for agrochemical delivery in the soil may be an important step forward in creating a more sustainable food system through the effective targeting of parasitic organisms and pests. Building on this work by assessing more types of soil and isolating the exact surface chemistry, soil properties, and particle sizes that affect mobility could be a fruitful area of research. Isolating some of these effects will allow for a more robust library of nanoparticles and computational approaches for predicting effective combinations of particles and soil for agrochemical delivery.

AUTHOR INFORMATION

Corresponding Author

Nicole F. Steinmetz − *Department of NanoEngineering, Department of Bioengineering, Department of Radiology, Moores Cancer Center, Center for Nano-ImmunoEngineering, Institute for Materials Design and Discovery, and Center for Engineering in Cancer, Institute for Engineering in Medicine, University of California San Diego, La Jolla, California 92093, United States;* orcid.org/0000-0002-0130-0481; Email: nsteinmetz@ucsd.edu

Authors

Udhaya Pooranam Venkateswaran − *Department of NanoEngineering, University of California San Diego, La Jolla, California 92093, United States*

Adam A. Caparco − *Department of NanoEngineering, University of California San Diego, La Jolla, California 92093, United States*

Ivonne González-Gamboa − *Department of NanoEngineering, University of California San Diego, La Jolla, California 92093, United States*

Reca Marian Caballero − *Department of Bioengineering, University of California San Diego, La Jolla, California 92093, United States*

Juliane Schuphan − *Institut für Molekulare Biotechnologie, RWTH Aachen University, 52074 Aachen, Germany;* orcid.org/0000-0002-9860-3058

Complete contact information is available at: https://pubs.acs.org/10.1021/acsagscitech.3c00074

https://doi.org/10.1021/acsagscitech.3c00074
ACS Agric. Sci. Technol. XXXX, XXX, XXX−XXX

Author Contributions

◆U.P.V. and A.A.C. contributed equally to this work.

Notes

The authors declare no competing financial interest.

■ ACKNOWLEDGMENTS

Dr. Jorge Leganes Bayon (UC San Diego) is acknowledged for providing PhMV (VLPs). This work was funded in part by a grant from USDA: NIFA-2020-67021-31255 (to NFS). Dr. Adam Caparco acknowledges a postdoctoral fellowship from USDA: NIFA 2022-67012-36698. This work was supported in part through the UC San Diego MRSEC, which is supported by the National Science Foundation under NSF Award Number DMR-2011924 (to NFS). The authors would like to thank the University of California, San Diego—Cellular and Molecular Medicine Electron Microscopy Core (UCSD-CMM-EM Core, RRID: SCR_022039) for equipment access and technical assistance. The UCSD-CMM-EM Core is supported in part by the National Institutes of Health Award number S10OD023527.

■ REFERENCES

(1) World Food Programme, https://www.wfp.org/global-hunger-crisis (accessed May 26, 2023).
(2) Tudi, M.; Daniel Ruan, H.; Wang, L.; Lyu, J.; Sadler, R.; Connell, D.; Chu, C.; Phung, D. T. Agriculture Development, Pesticide Application and Its Impact on the Environment. *Int. J. Environ. Res. Public Health* **2021**, *18*, 1112.
(3) Lowry, G. V.; Avellan, A.; Gilbertson, L. M. Opportunities and challenges for nanotechnology in the agri-tech revolution. *Nat. Nanotechnol.* **2019**, *14*, 517−522.
(4) Esse, H. P.; Reuber, T. L.; van der Does, D. Genetic modification to improve disease resistance in crops. *New Phytol.* **2020**, *225*, 70−86.
(5) DeRosa, M. C.; Monreal, C.; Schnitzer, M.; Walsh, R.; Sultan, Y. Nanotechnology in fertilizers. *Nat. Nanotechnol.* **2010**, *5*, 91.
(6) Raliya, R.; Saharan, V.; Dimkpa, C.; Biswas, P. Nanofertilizer for Precision and Sustainable Agriculture: Current State and Future Perspectives. *J. Agric. Food Chem.* **2018**, *66*, 6487−6503.
(7) Chariou, P. L.; Steinmetz, N. F. Delivery of Pesticides to Plant Parasitic Nematodes Using Tobacco Mild Green Mosaic Virus as a Nanocarrier. *ACS Nano* **2017**, *11*, 4719−4730.
(8) Nuruzzaman, M.; Rahman, M. M.; Liu, Y.; Naidu, R. Nanoencapsulation, Nano-guard for Pesticides: A New Window for Safe Application. *J. Agric. Food. Chem.* **2016**, *64*, 1447−1483.
(9) Cao, J.; Guenther, R. H.; Sit, T. L.; Lommel, S. A.; Opperman, C. H.; Willoughby, J. A. Development of Abamectin Loaded Plant Virus Nanoparticles for Efficacious Plant Parasitic Nematode Control. *ACS Appl. Mater. Interfaces* **2015**, *7*, 9546−9553.
(10) Wilhelm, S.; Tavares, A. J.; Dai, Q.; Ohta, S.; Audet, J.; Dvorak, H. F.; Chan, W. C. W. Analysis of Nanoparticle Delivery to Tumors. *Nat. Rev. Mater.* **2016**, *1*, 1−12.
(11) Yan, J.; Huang, K.; Wang, Y.; Liu, S. Study on Anti-Pollution Nano-Preparation of Dimethomorph and its Performance. *Chin. Sci. Bull.* **2005**, *50*, 108−112.
(12) Gupta, R.; Xie, H. Nanoparticles in Daily Life: Applications, Toxicity and Regulations. *J. Environ. Pathol., Toxicol. Oncol.* **2018**, *37*, 209−230.
(13) Santi, L.; Huang, Z.; Mason, H. Virus-like particles production in green plants. *Methods* **2006**, *40*, 66−76.
(14) Ma, Y.; Commandeur, U.; Steinmetz, N. F. Three Alternative Treatment Protocols for the Efficient Inactivation of Potato Virus X. *ACS Appl. Bio Mater.* **2021**, *4*, 8309−8315.
(15) Chariou, P. L.; Ma, Y.; Hensley, M.; Rosskopf, E. N.; Hong, J. C.; Charudattan, R.; Steinmetz, N. F. Inactivated Plant Viruses as an Agrochemical Delivery Platform. *ACS Agric. Sci. Technol.* **2021**, *1*, 124−130.
(16) Wen, A. M.; Steinmetz, N. F. Design of Virus-Based Nanomaterials for Medicine, Biotechnology, and Energy. *Chem. Soc. Rev.* **2016**, *45*, 4074−4126.
(17) Lomonossoff, G. P.; Wege, C. TMV Particles: The Journey From Fundamental Studies to Bionanotechnology Applications. *Adv. Virus Res.* **2018**, *102*, 149−176.
(18) Chariou, P. L.; Dogan, A. B.; Welsh, A. G.; Saidel, G. M.; Baskaran, H.; Steinmetz, N. F. Soil mobility of synthetic and virus-based model nanopesticides. *Nat. Nanotechnol.* **2019**, *14*, 712−718.
(19) Geiger, F. C.; Eber, F. J.; Eiben, S.; Mueller, A.; Jeske, H.; Spatz, J. P.; Wege, C. TMV nanorods with programmed longitudinal domains of differently addressable coat proteins. *Nanoscale* **2013**, *5*, 3808−3816.
(20) Masarapu, H.; Patel, B. K.; Chariou, P. L.; Hu, H.; Gulati, N. M.; Carpenter, B. L.; Ghiladi, R. A.; Shukla, S.; Steinmetz, N. F. Physalis Mottle Virus-Like Particles as Nanocarriers for Imaging Reagents and Drugs. *Biomacromolecules* **2017**, *18*, 4141−4153.
(21) Lee, K. L.; Uhde-Holzem, K.; Fischer, R.; Commandeur, U.; Steinmetz, N. F. Genetic engineering and chemical conjugation of potato virus X. *Methods Mol. Biol.* **2014**, *1108*, 3−21.
(22) Bagheri, I.; Kalhori, S. B.; Akef, M.; Khormali, F. Effect of Compaction on Physical and Micromorphological Properties of Forest Soils. *Am. J. Plant Sci.* **2012**, *03*, 159.
(23) Klug, A. The tobacco mosaic virus particle: structure and assembly. *Philos. Trans. R. Soc., B* **1999**, *354*, 531−535.
(24) González-Gamboa, I.; Caparco, A. A.; McCaskill, J. M.; Steinmetz, N. F. Bioconjugation Strategies for Tobacco Mild Green Mosaic Virus. *Chembiochem* **2022**, *23*, No. e202200323.
(25) Tiu, B. D. B.; Kernan, D. L.; Tiu, S. B.; Wen, A. M.; Zheng, Y.; Pokorski, J. K.; Advincula, R. C.; Steinmetz, N. F. Electrostatic layer-by-layer construction of fibrous TMV biofilms. *Nanoscale* **2017**, *9*, 1580−1590.
(26) Shukla, S.; Ablack, A. L.; Wen, A. M.; Lee, K. L.; Lewis, J. D.; Steinmetz, N. F. Increased Tumor Homing and Tissue Penetration of the Filamentous Plant Viral Nanoparticle Potato virus X. *Mol. Pharmaceutics* **2013**, *10*, 33−42.
(27) Wei, Y.; Cejas, C. M.; Barrois, R.; Dreyfus, R.; Durian, D. J. Morphology of Rain Water Channeling in Systematically Varied Model Sandy Soils. *Phys. Rev. Appl.* **2014**, *2*, No. 044004.
(28) White, S. M.; Tien, C. L. Analysis of flow channeling near the wall in packed beds. *Wärme - und Stoffübertragung* **1987**, *21*, 291−296.
(29) Flaischlen, S.; Kutscherauer, M.; Wehinger, G. D. Local Structure Effects on Pressure Drop in Slender Fixed Beds of Spheres. *Chem. Ing. Tech.* **2021**, *93*, 273−281.
(30) Hethcote, H. W.; DeLisi, C. Non-equilibrium model of liquid column chromatography: I. Exact expressions for elution profile moments and relation to plate height theory. *J. Chromatogr. A* **1982**, *240*, 269−281.
(31) Rogatsky, E. Pandora box of BCA assay. Investigation of the accuracy and linearity of the microplate bicinchoninic protein assay: Analytical challenges and method modifications to minimize systematic errors. *Anal. Biochem.* **2021**, *631*, No. 114321.
(32) Brewer, A.; Dror, I.; Berkowitz, B. The Mobility of Plastic Nanoparticles in Aqueous and Soil Environments: A Critical Review. *ACS ES&T Water* **2021**, *1*, 48−57.
(33) Zhu, C.; Wang, Q.; Huang, X.; Yun, J.; Hu, Q.; Yang, G. Adsorption of amino acids at clay surfaces and implication for biochemical reactions: Role and impact of surface charges. *Colloids Surf., B* **2019**, *183*, No. 110458.
(34) Mihayo, D.; Vegi, M. R.; Vuai, S. A. H. Attenuation of nitrate from aqueous solution using raw and surface modified biosorbents from Adansonia digitata fruit pericarp. *Heliyon* **2022**, *8*, No. e10004.
(35) Brancolini, G.; Rotello, V. M.; Corni, S. Role of Ionic Strength in the Formation of Stable Supramolecular Nanoparticle−Protein Conjugates for Biosensing. *Int. J. Mol. Sci.* **2022**, *23*, 2368.
(36) Sigmund, G.; Arp, H. P. H.; Aumeier, B. M.; Bucheli, T. D.; Chefetz, B.; Chen, W.; Droge, S. T. J.; Endo, S.; Escher, B. I.; Hale, S. E.; Hofmann, T.; Pignatello, J.; Reemtsma, T.; Schmidt, T. C.; Schönsee, C. D.; Scheringer, M. Sorption and Mobility of Charged

https://doi.org/10.1021/acsagscitech.3c00074
ACS Agric. Sci. Technol. XXXX, XXX, XXX−XXX

Organic Compounds: How to Confront and Overcome Limitations in Their Assessment. *Environ. Sci. Technol.* **2022**, *56*, 4702−4710.
(37) Laber, J. R.; Dear, B. J.; Martins, M. L.; Jackson, D. E.; DiVenere, A.; Gollihar, J. D.; Ellington, A. D.; Truskett, T. M.; Johnston, K. P.; Maynard, J. A. Charge Shielding Prevents Aggregation of Supercharged GFP Variants at High Protein Concentration. *Mol. Pharmaceutics* **2017**, *14*, 3269−3280.
(38) Cao, J.; Guenther, R. H.; Sit, T. L.; Opperman, C. H.; Lommel, S. A.; Willoughby, J. A. Loading and Release Mechanism of Red Clover Necrotic Mosaic Virus Derived Plant Viral Nanoparticles for Drug Delivery of Doxorubicin. *Small* **2014**, *10*, 5126−5136.
(39) Gerhardson, B.; Insunza, V. Soil Transmission of Red Clover Necrotic Mosaic Virus. *J. Phytopathol.* **1979**, *94*, 67−71.

https://doi.org/10.1021/acsagscitech.3c00074
ACS Agric. Sci. Technol. XXXX, XXX, XXX−XXX